Proceedings of the ASME 2024 19th International Manufacturing Science and Engineering Conference MSEC2024

June 17-21, 2024, Knoxville, Tennessee

MSEC2024-124108

BRIEF PAPER: QUANTIFYING SPATIAL HETEROGENEITY OF LAMINATED PEROVSKITE SEMICONDUCTORS USING PHOTOLUMINESCENCE MAPPING

Oluka Okia University of Michigan Ann Arbor, MI Clare Lanaghan University of Michigan Ann Arbor, MI Jack Palmer UC San Diego La Jolla, CA **Srinivas Yadavalli** University of Michigan Ann Arbor, MI

David Fenning UC San Diego La Jolla, CA Neil Dasgupta University of Michigan Ann Arbor, MI

ABSTRACT

Halide perovskite solar cells (PSCs) are a state-of-the-art photovoltaic technology that exhibit high efficiencies and can be manufactured using roll-to-roll systems. However, PSCs are currently fabricated using sequential layer-by-layer deposition, which constrains the selection of suitable functional layers in the solar cell and limits the processing conditions and techniques that can be used.

Lamination via diffusion bonding is a scalable parallel-processing technique that has the capability to overcome some of the challenges of sequential deposition by widening the thermal processing window and reducing the chemical compatibility requirements for PSC manufacturing. However, there remains a lack of detailed understanding of the process-structure-property relationships needed to accelerate the development of high-volume lamination-based manufacturing processes.

In this work, we introduce a method to study the process-structure-property relationships of laminated perovskite semiconductors by using a custom photoluminescence (PL) spectroscopy system to quantify spatial heterogeneity in laminated halide perovskite (HP) materials. PL is an important figure-of-merit used to quantify the optoelectronic properties of semiconductor materials used in PV manufacturing. The spatial variation in PL of a laminated HP film is compared to that of an unlaminated HP film.

The PL system uses servomotors and an Arduino microcontroller to automate a PL mapping procedure. The PL equipment is tunable to achieve a minimum possible spot size of $\sim 50~\mu m$, enabling high-resolution measurements. The system is used to measure the PL of 19 separate locations on both a laminated and unlaminated HP material.

The results of this study reveal that lamination at optimal conditions will improve the average PL peak intensity of the HP by 55%, indicating that lamination has the potential to improve the optoelectronic characteristics of PSCs. However, lamination also increases the standard deviation of PL peak intensity. Therefore, although lamination improves the PL of HPs, it also induces unwanted spatial heterogeneity. This warrants future studies on the governing physical mechanisms that determine quality control metrics in lamination-based PSC manufacturing.

Keywords: perovskite solar cells, solar energy, photoluminescence, metrology,

NOMENCLATURE

PSC Perovskite Solar Cell

L-PSC Laminated Perovskite Solar Cell

HP Halide Perovskite
PL Photoluminescence
R2R Roll-to-roll

R2R Roll-to-roll θ Angle (Degrees)

1. INTRODUCTION

Halide PSCs are an emerging low-cost photovoltaic (PV) technology that recently achieved a record-high power conversion efficiency of >26%, exceeding that of many other viable thin-film PV structures [1]. Unlike the most well-established PV technology, crystalline silicon, PSCs can potentially be fabricated using high-throughput and low-cost roll-to-roll (R2R) manufacturing methods, such as slot die coating and ink-jet printing [2]. However, despite their potential as a next-generation solar technology, poor long-term stability

and processing constraints are major factors limiting their commercial potential [3][4].

PSCs are commonly fabricated using sequential layerby-layer deposition, in which each functional material of the solar cell is deposited on top of the preceding layer until the device is complete. During sequential deposition, the processing methods for each new layer must be compatible with every layer beneath it. Therefore, sequential deposition often constrains the material selection for the functional layers in the solar cell and imposes limitations on the processing conditions used. For example, potential candidates for stable inorganic transport layer materials in PSCs, such as nickel oxide, often require high annealing temperatures that would thermally degrade the HP photoactive layer [5]. Additionally, the high-quality transport layer material tin oxide requires the use of aqueous precursors that will damage the perovskite layer if deposited on top of it. Furthermore, some manufacturing methods that could be useful for transport layer deposition, such as atomic layer deposition, require precursors that adversely affect HP layer. Therefore, these materials and methods are typically restricted to the bottom transport layer in a PSC device and are difficult to incorporate when depositing layers on top of the chemically and thermally sensitive HP material.

To overcome the processing challenges of sequential deposition, an alternative strategy is to use a lamination process, where two sub-components of the PSC can be fabricated in parallel and bonded together to complete a full PSC. A promising lamination approach, first proposed by Dunfield *et al.*, involves diffusion-bonding the two subcomponents of the PSC together at the HP-HP interface [3]. Lamination via diffusion bonding has the potential to improve stability by self-encapsulating the laminated perovskite solar cell (L-PSC) between two substrates (e.g. glass), which can prevent unwanted ingress of moisture and oxygen, both of which degrade the HP layer. Furthermore, diffusion bonding enables the use of materials and processing techniques that would normally degrade the HP layer if used during sequential deposition.

Although lamination offers several advantages as a scalable fabrication method for PSCs, a high-volume R2R manufacturing lamination process has not been demonstrated [6][7][8]. To demonstrate high-throughput R2R lamination of PCSs, it is important to experimentally study the influence of lamination parameters (e.g. pressure, temperature, dwell time) on the L-PSC microstructure, material properties, and device performance. However, full device fabrication is costly and time-consuming, necessitating the use of low-cost and high-throughput characterization techniques for data acquisition.

In this work, the process-structure-property relationships of laminated perovskite semiconductors are studied using a custom steady-state photoluminescence (PL) spectroscopy system. Specifically, the influence of lamination on the spatial homogeneity in PL of HP thin films is characterized.

PL is a useful characterization technique for PSCs because it is high-throughput, non-destructive, and low cost [9]. PL can be used to evaluate the presence of defects in HP thin films and PSC subcomponents, making it useful as an in-line metrology tool for a PSC manufacturing system [10][11]. Furthermore, the quasi-fermi level splitting, which determines the theoretical maximum open-circuit voltage in a PSC, is directly related to the photoluminescence quantum yield [9]. By assuming all optical coupling is constant across sampling points (a reasonable assumption), then the quasi-fermi level splitting, and thus the optoelectronic quality, of the absorber can be quantified and spatially resolved.

The PL system in this study uses a servomotor to enable movements for automated mapping. A separate servo is used to control the sample measurement conditions. Both servos are operated with an Arduino microcontroller, allowing for repeatable and controlled measurements. The PL equipment is tunable to achieve a minimum spot size of $\sim 50~\mu m$, enabling high-resolution measurements. The system is low-cost (<\$5,000), and has a modular design with swapable optical components, making it applicable as an in-line metrology tool.

2. MATERIALS AND METHODS

2.1 Perovskite Thin Film Deposition

 ${\sim}250 nm$ thick $FA_{0.8}MA_{0.15}Cs_{0.05}PbI_{2.6}Br_{0.4}$ HP thin films with 3 wt% excess lead iodide were prepared on glass substrates using a solution deposition approach. The bandgap of the HP films is 1.6 eV.

25mm x 25mm x 0.2mm glass substrates were cleaned in an ultrasonic bath of DI water for 10 minutes. Then, substrates were sonicated for 10 minutes in 3 separate baths of ethanol, acetone, and 2-propanol, respectively. Substrates were removed from the solvent bath and blow-dried with air for approximately 5 minutes. Substrates were then left to sit overnight before being cleaned with UV-ozone for 90 minutes.

The HP precursor solution was prepared by mixing 18 mg of Cesium Iodide (CsI; Fischer Scientific), 204.6mg of formamidinium iodide (FAI; Greatcell Solar), 23mg of methylammonium bromide (MABr; Greatcell Solar), 77mg of lead bromide (PbBr₂; Alfa Aesar), and 606.7mg of lead iodide (PbI₂; Fischer Scientific) in a solution of 1.6mL of dimethyl sulfoxide (DMSO; Sigma Aldrich, USA) and 0.4mL of dimethylformamide (DMF; Acros Organics, USA). Immediately after ozone cleaning, the substrates were loaded into a glovebox with an argon atmosphere to prepare for spin coating.

The substrates were spin-coated using a static spin-coating procedure. $\sim\!\!200~\mu L$ of HP precursor solution was first dropped onto the substrates with a pipette before being spun at 6000 rpm. 20 seconds after initiating spinning, the substrate is sprayed with $\sim\!\!200~\mu L$ of chlorobenzene (Sigma Aldrich, USA) and left to spin for 60 more seconds. Finally, the HP-coated substrates were annealed on a hot plate at 100 °C for 50 minutes.

2.2 Perovskite Lamination

The HP-coated glass substrates were laminated using a hydraulic hot-press and custom-designed jig. The jig and hydraulic press were heated to 150°C and given at least 10 minutes to reach steady state. The first HP-coated substrate was

loaded into the jig with the HP film facing upwards (face up). The second HP-coated substrate was placed face down on top of the first HP-coated substrate, allowing the two HP films to contact each other. The jig with samples was loaded into the hydraulic press and given 5 minutes to come to the steady-state temperature of 150°C. Next, a pressure of 5.5 MPa was applied for a duration of 10 minutes, allowing the HP layers to join through a diffusion-bonding process (Figure 1). The jig was unloaded and given 4 minutes to cool down before removing the samples.

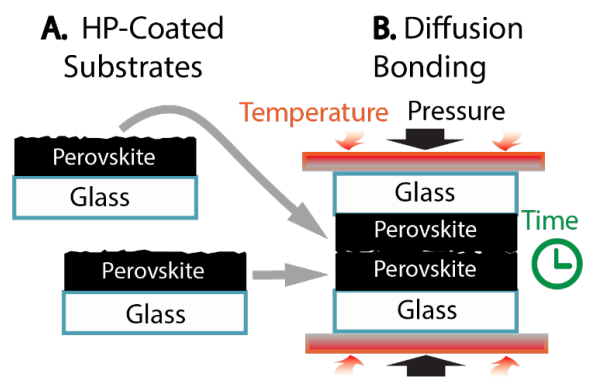


FIGURE 1: LAMINATION PROCESS OF HP-COATED SUBSTRATES

2.3 Photoluminescence Mapping Procedure

PL mapping was carried out using the custom-designed PL system shown schematically in Figure 2. The system uses a $\sim\!520$ nm class II laser to excite the HP film. It is known that ion mobility, and therefore phase segregation, scales with light intensity in HP materials [12]. Therefore, to minimize changes in sample nanostructure due to ion migration, the laser light intensity was kept below 1-sun by tuning the laser spot size to $\sim\!1$ mm. However, it is possible to achieve a minimum spot size of $\sim\!50~\mu m$.

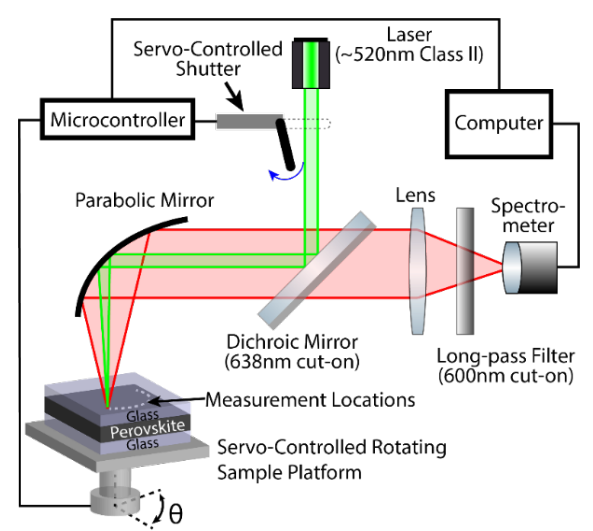


FIGURE 2: SCHEMATIC OF CUSTOM PL MAPPING SYSTEM. θ IS THE ANGLE AT WHICH THE SERVO HAS ROTATED TO ACHIEVE A PL MEASUREMENT AT A NEW LOCATION.

To perform a PL map, the sample is placed on the servocontrolled rotating platform. The laser is turned on and a servocontrolled shutter opens, exposing the sample to the laser for 5 seconds. Then, luminescence from the sample is collected, filtered by a series of optics, and is ultimately sent to a compact spectrometer (CCS200, Thorlabs). It is important to use the servo shutter to control the duration of time that the laser shines on the sample because HPs exhibit a time-dependent steady-state PL response to photoexcitation [13]. After the PL spectra is processed by the spectrometer, it is normalized to the integration time of the spectrometer. Next, the servo-controlled rotating platform rotates the sample to a new location and the PL collection procedure is repeated. The rotation process is illustrated in Figure 2, where θ is the total angle that the servo has rotated to measure PL at a new location. The process is repeated 19 more times to collect PL at 20 different locations on a sample, forming an arc. A single arc-scan is defined as one of the four curved lines making the star-shaped array of measurement points seen in Figure 3B. To generate Figure 3A, 80 locations are measured by repositioning the orientation of the sample on the sample platform by 90 degrees three times and taking an arc scan each time. A single servo was used to enable single-axis PL mapping for the first iteration of the design. Because the servo motor in the sample platform is designed for rotational motion, it causes the sample to rotate along the arc of a circle, as shown in Figure 2. Future designs will incorporate multi-axis position control using linear stages. The approximate positions of each sample location are shown overlayed on a digital microscope image (VHX 7100, Keyence Corp) of the sample in Figure 3B.

An Arduino microcontroller synchronizes the servo-controlled rotating platform and the servo-controlled shutter. The Arduino microcontroller and spectrometer are synchronized using a custom python software package on an external computer. An unlaminated sample is characterized using the same procedure as the laminated sample. However, unlike the laminated sample, the two HP-coated substrates of the unlaminated sample were placed face to face on the stage and were not diffusion bonded together. To validate our custom PL setup, PL traces were taken from the same laminated sample using our custom PL setup and a spectrofluorometer (Horiba Fluorolog-QM), which were in good agreement.

3. RESULTS AND DISCUSSION

In Figure 3A, the PL intensity values for each location measured on a sample are plotted. The approximate measurement coordinates are shown overlayed onto a digital microscope image of the sample in Figure 3B. Significant spatial variation in PL was observed, with PL values ranging from 0.7 to 17.5 (a.u).

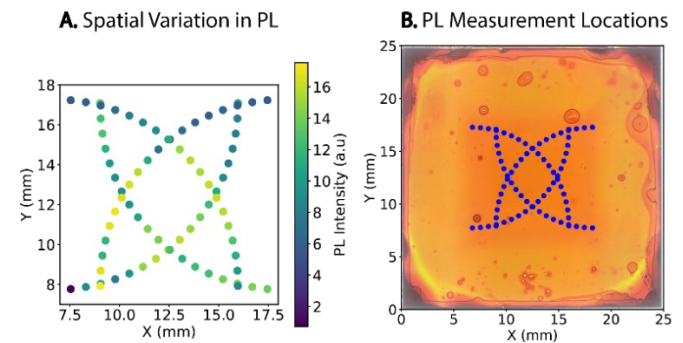


FIGURE 3: A) PL MAP OF A LAMINATED SAMPLE, B) PL MEASUREMENT LOCATIONS OVERLAYED ON DIGITAL MIRCORSCOPE IMAGE OF THE HP SAMPLE

To further understand the impact of lamination on spatial variation, the PL intensity of a laminated HP sample is compared to that of an unlaminated HP sample for an individual arc scan (Figure 4). To prepare the unlaminated sample, the same spin-coating and annealing procedures were used. The two substrates were placed on top of each other face-to-face without being laminated, and were subsequently characterized via PL. Overall, the lamination process increases the mean PL intensity by 55%, which suggests an improvement in optoelectronic quality of the HP material. However, lamination also causes an increase in the standard deviation of PL intensity (Table 1).

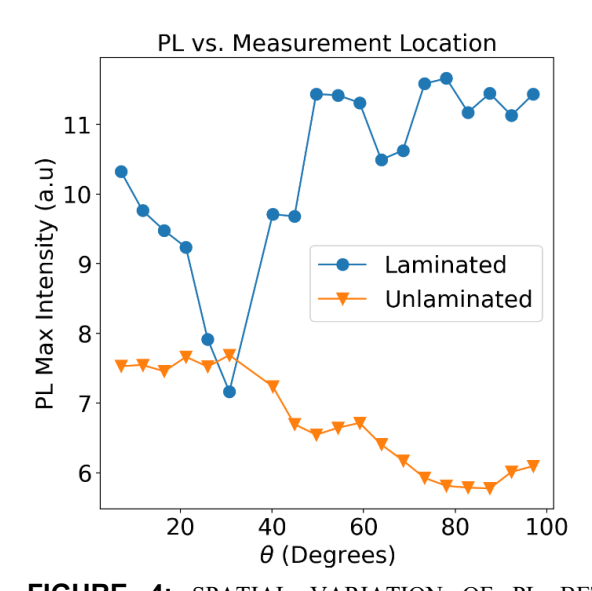


FIGURE 4: SPATIAL VARIATION OF PL BETWEEN A LAMINATED AND UNLAMINATED SAMPLE FOR AN ARC SCAN. θ REPRESENTS THE SERVO ANGLE OF ROTATION AND IS SHOWN IN FIGURE 2.

	PL (a.u.): Laminated	PL (a.u.): Unlaminated
Mean	10.4	6.7
Standard	1.3	0.7
Deviation		

Table 1: STATISTICAL COMPARISON OF SPATIAL VARIATION IN PL INTENSITY OF A LAMINATED AND UNLAMINATED HP SAMPLE FOR AN INDIVIDUAL ARC SCAN

The results of this study show that the diffusion bonding process causes an overall improvement in the average steady-state PL intensity of an HP material. One potential reason for the observed increase in PL is an increase in the grain size of the laminated HP. Previous studies have shown grain growth in HP materials subject to elevated temperature and pressure during lamination [7][8]. Grain boundaries have been shown to be primary sites for non-radiative recombination, with larger grains yielding a greater power conversion efficiency (PCE) in PSCs [10]. PL is emission caused by radiative recombination.

Despite the overall improvement in PL intensity, diffusion bonding also caused an undesirable increase in the spatial heterogeneity of the laminated HP. However, while the absolute value of the standard deviation in PL increased substantially, the increase was smaller when normalizing the standard deviation to the mean. Specifically, the coefficient of variations for the unlaminated and laminated samples are 54% and 64%, respectively. There are several potential causes for this increase that warrant further study, including non-uniform pressure and temperature distributions over the HP sample and spatial heterogeneity in the phase or microstructure of the material.

The findings of this study motivate several directions for future work. The underlying physical and chemical mechanisms causing the increase in PL and spatial heterogeneity in PL need to be correlated with performance of PSCs. Additionally, the PL mapping system in this study will be upgraded to a 2-axis motorized stage, allowing for more complete coverage of the HP surface.

Understanding the mechanisms controlling spatial evolution of the HP microstructure and optical properties during lamination will provide insight into the key parameters to control when designing future R2R fabrication systems of PSCs. Ultimately, understanding how to eliminate spatial heterogeneity in laminated PSCs will allow higher performing devices to be fabricated using lamination processes.

4. CONCLUSION

In this study, the influence of lamination on the spatial heterogeneity of HP semiconductors was quantified using a low-cost automated steady-state photoluminescence (PL) system. It was found that although lamination causes a desirable increase in average PL, it also causes an undesirable increase in spatial heterogeneity of PL. In the future, this platform will be used for metrology during lamination-based manufacturing of PSCs.

ACKNOWLEDGEMENTS

This work was supported in part by the U.S. Department of Energy's Office of Energy Efficiency and Renewable Energy (EERE) under Solar Energy Technologies Office (SETO) agreement number EE-0009521. This material is based upon work supported by the National Science Foundation under grant no. 2328010. O.O. and C.L. acknowledge support from the National Science Foundation Graduate Research Fellowship

Program under grant no. DGE-1256260.

REFERENCES

- [1] J. Park et al., | Nature |, 2023
- [2] Z. Li et al., Nature Reviews Materials, 2018
- [3] S. P. Dunfield et al., ACS Energy Lett, 2018
- [4] S. P. Dunfield et al., Advanced Energy Materials, 2020
- [5] T. Bin Song et al., J Mater Chem A Mater, 2015
- [6] T. Li, W. A. Dunlap-Shohl, and D. B. Mitzi, ACS Appl Energy Mater, 2020
- [7] W. A. Dunlap-Shohl, T. Li, and D. B. Mitzi, *ACS Appl Energy Mater*, 2019
- [8] S. K. Yadavalli et al., ACS Appl. Mater. Interfaces. In Press, 2024.
- [9] T. Kirchartz, J. A. Márquez, M. Stolterfoht, and T. Unold, *Advanced Energy Materials*, 2020
- [10] X. Lin et al., Adv Funct Mater, 2018
- [11] C. Li, A. Guerrero, S. Huettner, and J. Bisquert, *Nature Communications*, 2018
- [12] E. T. Hoke, D. J. Slotcavage, E. R. Dohner, A. R. Bowring, H. I. Karunadasa, and M. D. Mcgehee, *Chem. Sci.*. 2015
- [13] N. S. Mahon et al., Solar Energy, 2020